



OPEN **Imply on diagnosis and early prognosis of preoperative [⁶⁸Ga]Ga-PSMA-11 PET/CT in patients with suspected brain tumours of glial origin**

K. Pełka^{1,2}✉, K. Koczyk^{3,4}, L. Koperski⁵, T. Dziedzic³, A. Nowak³, L. Królicki¹, P. Kunert³ & J. Kunikowska¹

PET/CT targeting prostate-specific membrane antigen (PSMA) is commonly used in patients with prostate cancer. PSMA has been found in other solid tumours, including primary brain tumours. The aim of this study was to evaluate the usefulness of [⁶⁸Ga]Ga-PSMA-11 PET/CT for preoperative diagnosis and 2-year prognosis. We prospectively screened patients with suspected glioma tumour. The PET/CT qualitative and quantitative results were compared to the histopathological examination. We compared glioblastoma (GBM) diagnostic data or between high-grade (HGG) and low-grade (LGG) gliomas. Overall (OS) and progression free survival (PFS) were analysed. Forty-four patients met the inclusion criteria. Twenty of them had positive and twenty-four negative scans. The sensitivity, specificity, positive predictive value, and negative predictive value for HGG diagnosis were 71.4 (95% confidence interval – 51.3–86.8), 100.0 (79.4–100.0), 100.0 (83.1–100.0), and 66.7 (44.7–84.4), respectively. For differentiation between GBM vs non-GBM tumours, the best parameter was the tumour-to-background ratio, with the area under the receiver operating characteristic curve 0.81 (0.66–0.96; 42.2) (95% CI; cut-off). Patients with positive PET/CT scans had similar PFS and OS to patients with HGG. PSMA accumulation negatively affected the PFS and OS of patients with diagnosed GBM. [⁶⁸Ga]Ga-PSMA-11 PET/CT showed optimistic diagnostic results and may be prognostic a factor.

Registration at www.clinicaltrials.gov 09/06/2023 with number NCT05896449.

Keywords [⁶⁸Ga]Ga-PSMA-11, PSMA PET/CT, Glioblastoma, GBM; primary glial tumour

Prostate-specific membrane antigen (PSMA) is a membrane protein that is encoded by the folate hydrolase 1 gene in humans¹. Compared with other imaging methods, PSMA plays a role in the wide diagnosis of patients with prostate cancer with the highest sensitivity and specificity². Intracranial PSMA expression has been found on solid neoplasms of origins other than prostate cancer, including primary brain tumours^{3–9}; metastases of the lung and breast; thyroid carcinoma; meningiomas; dermoid cysts; and primary juvenile nasal angiofibroma¹⁰. It has also been found in nonmalignant lesions such as stroke, neurocysticercosis or tuberculosis¹⁰. Its occurrence is linked to neovascularization¹¹. There are no data on the prognostic value of PSMA expression in intracranial tumours.

Diffuse gliomas are the most prevalent malignant primary brain tumours in adults. These tumours are classified according to the 5th edition of the World Health Organization (WHO) Classification of Tumours of the Central Nervous System (2021)¹² based on histopathological examination combined with molecular testing. Adult-type diffuse gliomas comprise three distinct types: astrocytoma, IDH-mutant, oligodendroglioma, IDH-mutant and 1p/19q-codeleted, and glioblastoma, IDH-wildtype. The histopathological grading of malignancy (WHO G2–G4) was maintained within types. Traditionally, these tumours are divided into low-grade (LGG) (WHO G2) and

¹Nuclear Medicine Department, Medical University of Warsaw, Banacha 1a, 02-097 Warsaw, Poland. ²Laboratory of Centre for Preclinical Research, Department of Research Methodology, Medical University of Warsaw, Warsaw, Poland. ³Department of Neurosurgery, Medical University of Warsaw, Warsaw, Poland. ⁴Doctoral School, Medical University of Warsaw, Warsaw, Poland. ⁵Department of Pathology, Medical University of Warsaw, Warsaw, Poland. ✉email: kacper.pelka@wum.edu.pl

high-grade (HGG) gliomas (WHO G3 and G4). Glioblastomas, IDH-wildtype (GBMs) are the most common primary diffuse gliomas and have the highest grade of malignancy. Microvascular proliferation and necrosis are hallmark histopathological features of GBMs¹³, yet the 5th edition of the WHO Classification allows for a diagnosis of GBM to be made in patients with specific genetics features, in absence of these histopathological features¹⁴. Surgery has been established as the primary treatment for diffuse gliomas. Preoperative prediction of tumour localisation, type, grading and the condition and age of patient is crucial for deciding on eligibility for surgery, better surgical planning of resection and potential use of oncological treatment.

The main diagnostic modality for diffuse gliomas is magnetic resonance imaging, but its ability to predict histopathological diagnosis is limited; thus, developing new modalities for preoperative imaging is vital. Several studies have confirmed that PET/CT with different tracers can play a significant role in future diagnostics. Depending on the tracer used, the final result can be based on various factors, such as glucose metabolism¹⁵, neovascularization, amino acid transport systems (¹¹C]MET has a sensitivity 75–100% and specificity 70–100% of differentiation recurrence of gliomas from radiation necrosis and ¹⁸F]FET PET has a sensitivity of 71–80% and a specificity of 56–85% for the differentiation between HGG and LGG)^{16–18}, and neuroinflammation¹⁹. These markers have advantages and disadvantages, such as the high availability and low cost of ¹⁸F]FDG, which is associated with high accumulation in normal brain tissues. And ¹⁸F]FLT which is expensive and difficult to access, and its sensitivity and specificity reaches 100%, compared to ¹⁸F]FDG where it reaches 70 and 100 respectively.

The usefulness of PSMA PET/CT for detecting glioblastoma recurrence has been confirmed by several publications^{9,20,21}. It may be radiolabelled with ¹⁸F or ⁶⁸Ga, which makes it accessible. Another advantage is the exceptionally low accumulation in brain tissues, which allows for significant differences between the accumulation in the tumour and the surrounding tissue²². A recently published meta-analysis provided consistent data for the correlation between radionuclide uptake and HGG diagnosis: sensitivity 98.2% (95% CI: 75.3–99.9%), specificity 91.2% (95% CI: 68.4–98.1%), likelihood ratio + (LR+) 4.5 (95% CI: 2.2–9.3), likelihood ratio- (LR-) 0.07 (95% CI: 0.04–0.15), and diagnostic odds ratio (DOR) 70.1 (95% CI: 19.6–250.9)²³. Unfortunately, these findings are based on a small number of studies, some of which involve recurrence rather than primary diagnosis. In our experience, the occurrence of PSMA uptake during recurrence is often associated with progression to more malignant tumours²⁴. Therefore, studies on patients with suspected disease are still needed to determine the clinical usefulness and impact on prognosis.

This study aimed to analyse the impact of ⁶⁸Ga]Ga-PSMA-11 PET/CT in preoperative differentiation of tumour type and grading in patients suspected of having a tumour of glial origin based on previously performed imaging examinations and to assess whether ⁶⁸Ga]Ga-PSMA-11 PET/CT result is associated within early survival of at least 2-years follow-up data.

Materials and methods

Study design

A prospective study was designed to compare the preoperative ⁶⁸Ga]Ga-PSMA-11 PET/CT results with the final histopathological diagnosis and at least 2-years follow-up.

Due to the small amount of data available, the study was conducted as a pilot study, and future studies in terms of group size will be designed based on these results. During this study, it was assumed that at least 40 patients should be assessed to result in groups of at least 10 patients with WHO stage 2, 3 and 4.

Participants

The patients were recruited from those who were referred to the department of neurosurgery, with suspicion of diffuse glioma in previously performed imaging studies. Sixty patients were screened between June 2020 and May 2022.

The inclusion criteria were:

- primary lesion found via MRI with radiological features of glial neoplasm
- untreated disease, planned surgery
- a negative medical history of other neoplastic diseases
- age older than eighteen
- informed, voluntary consent to participate in the study

The exclusion criteria were as follows:

- pregnant women, breastfeeding women
- persons with a known allergy to PSMA
- age under eighteen
- patient's lack of cooperation

The study was approved by the local Medical University of Warsaw Bioethics Committee (protocol number KB/2/A/2018 and KB/177/2021). All the subjects provided written informed consent. The study has been registered at clinicaltrials.gov (number: NCT05896449) at 09/06/2023.

Figure 1 presents the study schema concept.

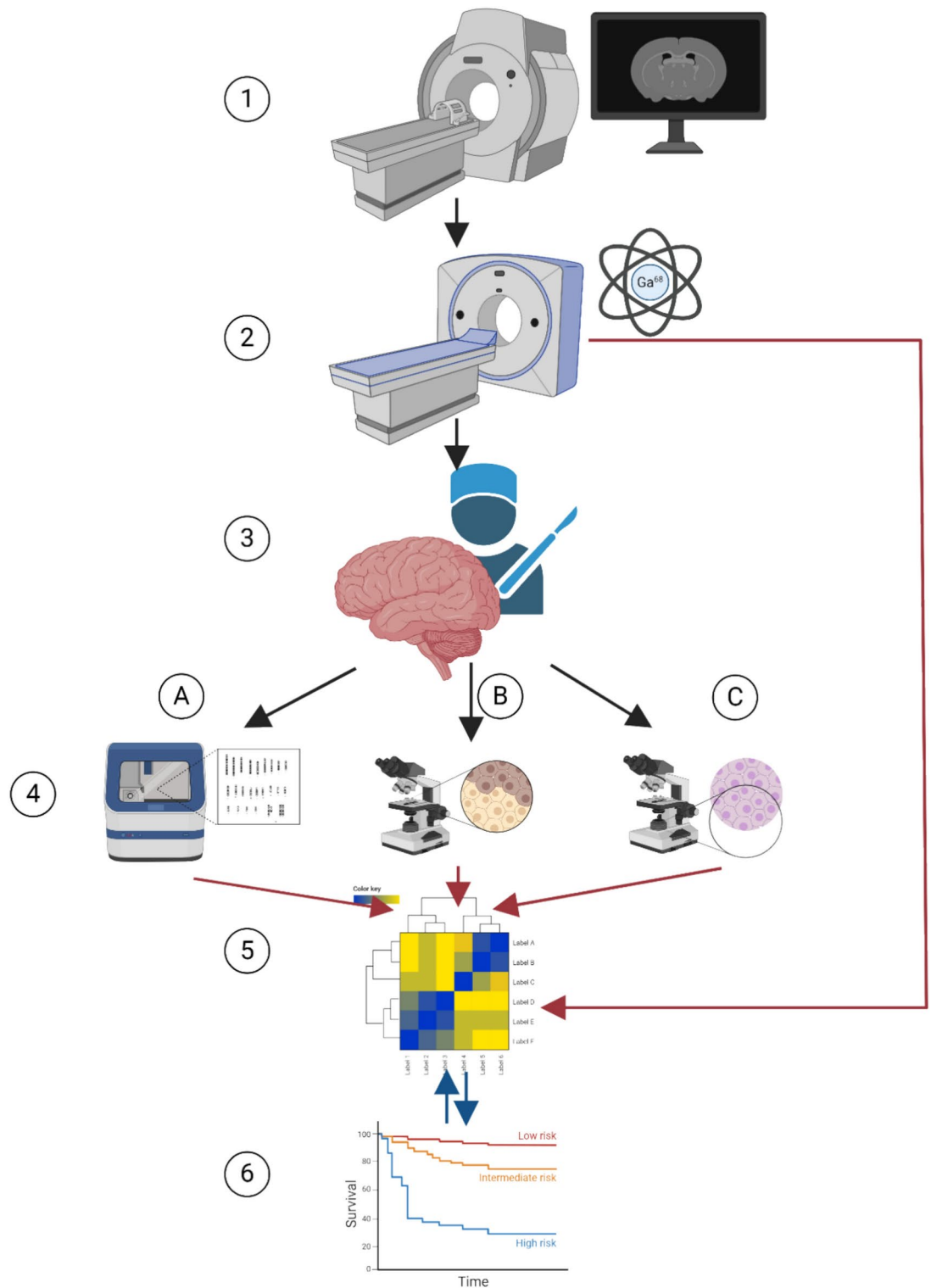


Fig. 1. Study concept. 1 – Patients with a suspected glial tumour on conventional imaging that required surgery were assessed for the study; 2 – presurgical PET/CT with $[^{68}\text{Ga}]\text{Ga-PSMA-11}$; 3 – neurosurgical resection; 4 – analysis of the collected material A – genetic analysis; B – immunohistochemical analysis C – standard histopathological analysis; 5 – statistical analysis of the collected data; 6 – follow-up with statistical analysis. Created in BioRender. Wlodarski, P. (2024).

Test methods

[⁶⁸Ga]Ga-PSMA-11 PET/CT protocol and image interpretation

A PSMA-11 kit containing 20 µg of PSMA-11 (Glu-CO-Lys(Ahx)-HBED-CC) and 60 mg of sodium acetate (POLATOM, Poland) and eluates from a ⁶⁸Ge/⁶⁸Ga GalliaPharm generator (Eckert&Ziegler, Germany) was used for the [⁶⁸Ga]Ga-PSMA-11 preparation.

Due to the study protocol PET/CT image acquisition was performed from the skull to the mid-thigh (3 min per bed position, 3 iterations, 21 subsets) with a CT scan (120 kV, 170 mAs reference) with dose modulation for anatomic correlation (CARE dose 4D) and attenuation correction on a Biograph 64 TruePoint (Siemens Medical Solutions, Inc., USA) 60 min postinjection of [⁶⁸Ga]Ga-PSMA-11 (2 MBq per kg body weight) with an additional 5 min of acquisition was used for brain imaging (one bed position).

Image analysis was performed using a Siemens Workstation (Syngovia, MMWS, Siemens Medical Solutions, Inc., USA). The PET/CT scans were analysed by two nuclear medicine physicians (with three and eight years of experience in PSMA PET/CT reading). The physicians had access to all the clinical data except the histopathological examination results when describing the study.

On visual evaluation, any cerebral focal uptake not associated with normal anatomical structures was interpreted as a positive lesion. For quantitative analysis, the maximal standard uptake value (SUV_{max}) and mean standard uptake value (SUV_{mean}) of each positive lesion were measured using the volume of interest (VOI) with a 10% percent cut-off. The target-to-background ratios (TBRs) were calculated using the SUV_{max} of the lesion divided by the SUV_{max} of the background measured using a similar size VOI placed in contralateral hemisphere in an unaffected region, representing normal brain tissue. Target-to-liver background ratios (TLRs) were calculated by dividing the SUV_{max} of the lesion by the SUV_{mean} of the spherical VOI placed in the right lobe of liver.

Postoperative histopathological and genetic examinations

The tissue collected during the surgery underwent histopathological examination at the Medical University of Warsaw Department of Pathology with a standard histopathological procedure according to pathomorphological guidelines for the assessment of tumours of glial origin. Histopathological examination was performed by a pathologist with at least 5 years of experience. All the clinical data were available to the pathologists. Genetic testing via next-generation sequencing (NGS) analysis was conducted by a genetic department upon additional written informed consent. The histopathological diagnosis incorporating the results of standard microscopic examination, molecular classification and genetic testing was formulated by an experienced pathologist and included in the study.

PSMA immunostaining

Immunostaining was performed to obtain additional data regarding PSMA expression in the collected material²⁵. Tissue fragments obtained during surgery were cut into 4-µm sections from paraffin blocks and placed on glass slides. Next, the sections were deparaffinized with xylene and dehydrated with gradient alcohol. Subsequently, antigen retrieval was performed at high temperature and pressure in citrate buffer (pH 9.0). Sections were incubated with primary PSMA antibody (mouse Mba, Dako/Agilent, Clone 3E6; dilution 1:50). A prostate cancer sample was used as a positive control. EnVision FLEX was used for visualization of the staining. All sections were then counterstained with hematoxylin. The immunohistochemically stained slides were scanned with a Hamamatsu NanoZoomer 2.0-HT scanner, viewed using NDP.view2 software and subsequently evaluated. All procedures were performed according to the manufacturer's instructions.

The immunoreaction of the endothelium and tumour cells was analysed. A score was assigned semiquantitatively based on staining intensity and distribution as follows: 0, negative; 1, faint and weak staining at high power; 2, moderate intensity at low power; and 3, strong reaction at low power. When there was heterogeneity in the intensity of staining, the score was considered based on the predominant pattern. The staining was performed on the available material, as described in the relevant paragraph.

Pre-surgical MRI

Prior to surgery, patients underwent imaging studies—most commonly T1-weighted MRI without and with contrast, T2-weighted MRI with fluid-attenuation inversion recovery (FLAIR) imaging, diffusion and spectroscopy MRI. The results were analysed by two radiologists with at least 8 years of experience in brain MRI studies.

Follow-up

Till now a follow-up was carried out at least 2-years after the operation in a group of available patients. Tumour progression was defined according to the RANO criteria using contrast-enhanced MR. Whenever possible, the date of the first MR showing progression was used to calculate progression-free survival (PFS). In a few patients in whom a clear clinical deterioration was present, but no MR was performed, an estimated date of clinical deterioration was used to calculate PFS. Overall survival (OS) was determined by the time of patient death.

Statistical analysis

To estimate the predictive value of [⁶⁸Ga]Ga-PSMA-11 PET/CT in comparison to that of histopathological examination, a contingency table was used. The results were analysed via qualitative and quantitative assessments. To obtain the cut-off parameters for the quantitative values, area under the curve (AUC) and receiver operating characteristic (ROC) curves were prepared and analysed. Student's t test was used to compare physiological accumulation between groups. Comparisons of the data with additional immunohistochemical staining were performed by chi-square and Spearman's rank-order correlation coefficient tests for qualitative analysis.

To analyse the follow-up data, the Kaplan–Meier estimator was used with the F-Cox and chi-square tests to compare the data between two or more groups. The statistical analyses were performed using PQStat v.1.8.4.152 (PQStat Software, Poznań, Poland) and Statistica v.13 (StatSoft Polska, Kraków, Poland). Due to the analysis of only possible patients for inclusion, without direct comparison to the general population, the results regarding sensitivity and specificity are not a direct reflection of the original sensitivity and specificity of the test for disease detection.

The datasets generated during and/or analysed during the current study are available from the corresponding author upon reasonable request.

Results

There were 159 patients with adult-type diffuse gliomas treated at the Department of Neurosurgery between 06/2020 and 05/2022; 89 were male (56%), and seventy were female (44%), with a median age of 51 (range 18–82). Due to the availability of PET/CT and operating theatre, we were able to assess 60 patients, 35 were male (58%), and 25 were female (42%), with a median age of 40.5 (range 21–73), 54 of whom met the inclusion criteria and had [⁶⁸Ga]Ga-PSMA-11 PET/CT scans (because of a technical problem with the scanner, 2 patients had [⁶⁸Ga]Ga-PSMA-11 PET/CT scans only of the head because the negative scan results did not affect the collected data). Of the remaining 54 patients, 2 patients declined surgery, and three were disqualified from surgery due to suspicion of stroke (1 patient) or demyelinating lesions (2 patients). The remaining patients (49 patients) underwent surgical resection of the tumour mass with curative purpose. After surgery, five patients were excluded from the analysis because of histopathological results: lack of tumour tissue (3 patients: 1 with demyelinating lesion resembling Baló concentric sclerosis, 1 with HIV-related inflammatory changes with necrosis and 1 with normal brain tissue), diffuse midline glioma, H3 K27M-altered (1 patient), or adenocarcinoma metastasis (1 patient). Finally, a statistical analysis was conducted on a group of 44 patients with twenty-positive and twenty-four negative [⁶⁸Ga]Ga-PSMA-11 PET/CT images. The flowchart of the study is presented in Fig. 2.

The tumour samples for genetic testing were collected from all patients included in the analysis as a part of histopathological examination. The detailed characteristics of the patients are given in supplementary material 1.

[⁶⁸Ga]Ga-PSMA-11 PET/CT

The [⁶⁸Ga]Ga-PSMA-11 PET/CT scan was performed in 54 patients. No related radiopharmaceutical side effects have been reported. The median time between the [⁶⁸Ga]Ga-PSMA-11 PET/CT scan and surgery was 2 days (range 0–70; quartile 25%–75%: 2–7).

According to our visual analysis, there were no inconclusive findings. Moreover, there were no significant differences in the physiological uptake of PSMA between the patients.

[⁶⁸Ga]Ga-PSMA-11 PET positive lesions

As a first step of the study, qualitative image analysis was performed. Focal increased tracer accumulation was found in 20 patients. The characteristics of patients with foci of increased accumulation are presented in supplementary material 2. The median accumulation values were as follows: SUVmax, 6.9; SUVmean, 4.0; volume, 24.3 cm³; TBR, 72.2; and TLR, 1.3.

Within the [⁶⁸Ga]Ga-PSMA-11 PET positive patients, we found only patients with HGG, with the following histological diagnoses: 5 patients with oligodendroglioma, IDH-mutant, and 1p/19q-codeleted (WHO G3 – 5); 4 patients with astrocytoma and an IDH-mutant (WHO G3 – 2, G4 – 2); and 11 patients with GBM and an IDH-wildtype (WHO G4 – 11). Among patients with GBM, microvascular proliferation and necrosis were diagnosed in samples from all the patients, prompting a GBM diagnosis based on histopathological criteria. The sample images are presented in Fig. 3.

[⁶⁸Ga]Ga-PSMA-11 PET negative lesions

On [⁶⁸Ga]Ga-PSMA-11 PET, 24 patients had no uptake in the brain. In this cohort, we found 16 patients with LGG and 8 patients with HGG. Patients had astrocytoma, IDH-mutant WHO G2-8 patients and WHO G3-3 patients; oligodendroglioma, IDH-mutant, and 1p/19q-codeleted WHO G2-8 patients and WHO G3-2 patients; and glioblastoma, IDH-wildtype WHO G4-3 patients. In all three patients with glioblastoma, tumours were initially diagnosed as IDH-wildtype diffuse gliomas or astrocytomas because there was no microvascular proliferation or necrosis in their histopathological examination. Only after the results of genetic analyses were the molecular features of glioblastoma identified; thus, the diagnosis and grading were improved accordingly. In one case in NGS study only TERT mutation has been found, in other apart from TERT mutation there was monosomy of 10. chromosome and additional 7. chromosomes. The sample images are presented in Fig. 3.

Other tumours—Nonprimary diffuse adult gliomas group (n = 5)

The final histopathological diagnosis in five patients after surgery did not confirm an adult-type diffuse glioma.

Two of them had positive [⁶⁸Ga]Ga-PSMA-11 PET results: histopathological examination revealed metastasis from lung adenocarcinoma (1 patient) and a demyelinating lesion resembling Baló concentric sclerosis (1 patient).

The other three patients had negative [⁶⁸Ga]Ga-PSMA-11 PET scans, and the following histopathological results were obtained: diffuse midline glioma H3 K27M-altered (WHO G4), which is representative of paediatric-type diffuse high-grade gliomas (1 patient); HIV-related inflammatory changes with necrosis (1 patient); and normal brain tissue (1 patient).

Due to the inclusion criteria, the data of these patients were not included in the statistical analysis. The sample images are presented in supplementary material 3.

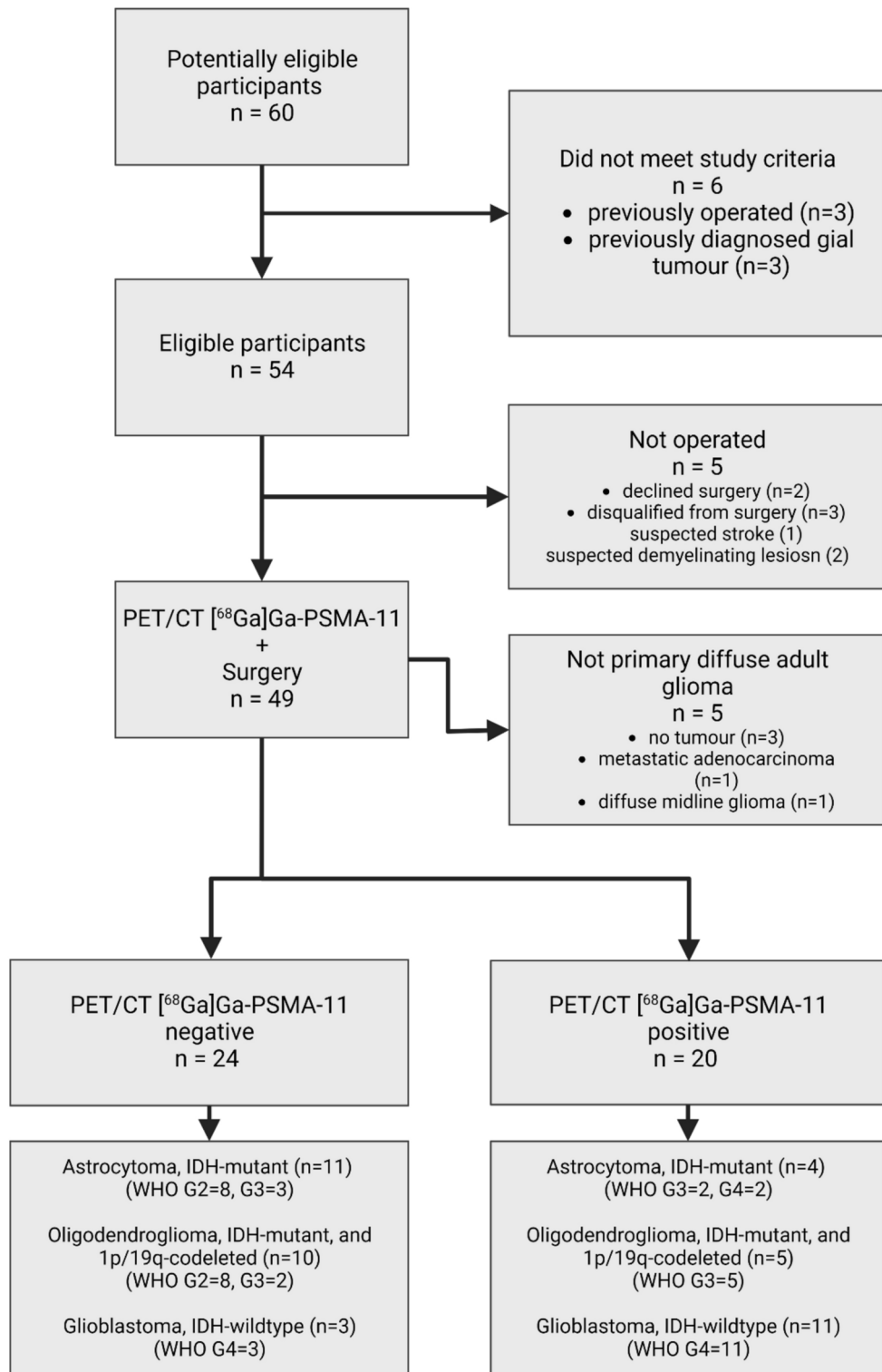


Fig. 2. Flow of participants.

Test results

Qualitative analysis

We analysed the qualitative results of [^{68}Ga]Ga-PSMA-11 PET compared to the histopathological examination results to determine the sensitivity, specificity, positive predictive value (PPV), negative predictive value (NPV), LR+, LR– and DOR for differentiating HGG vs LGG, glioblastoma vs nonglioblastoma and WHO G4 vs WHO G2 + G3 gliomas. The results are presented in Table 1 with 95% confidence intervals (CIs).

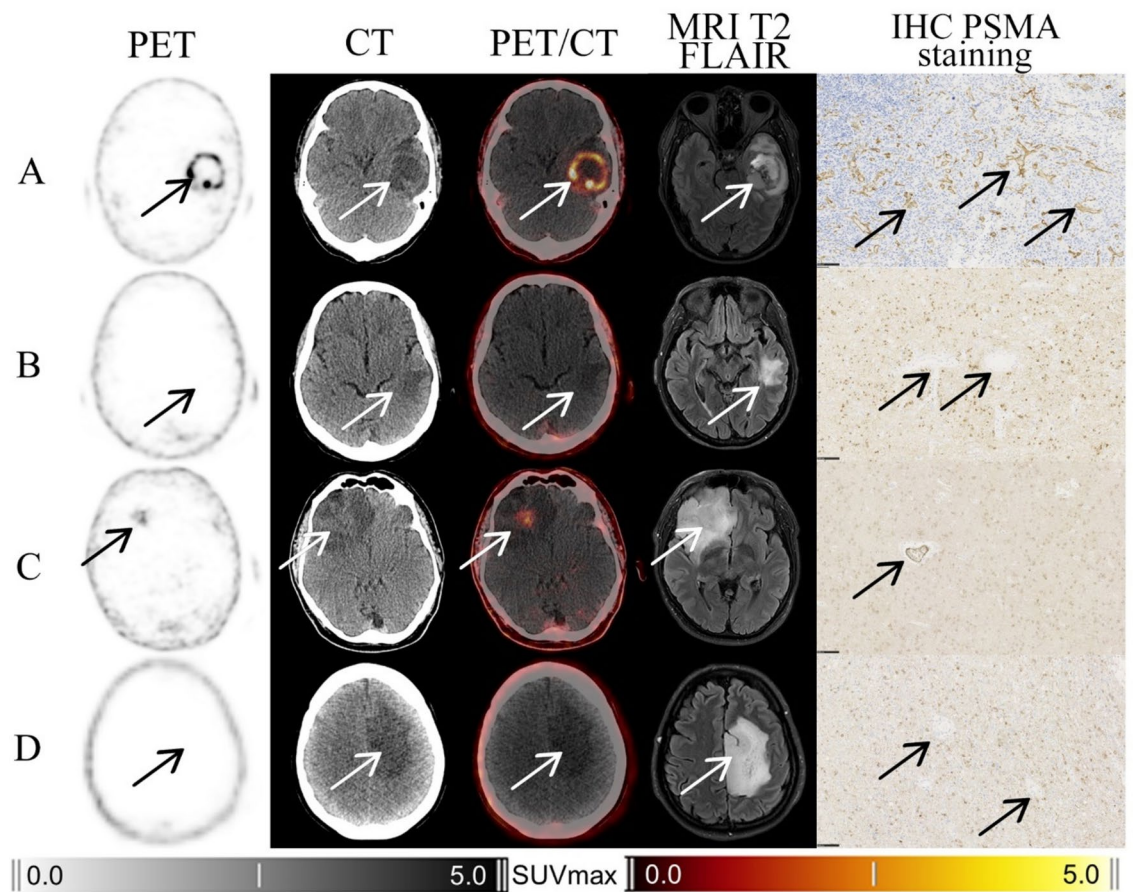


Fig. 3. Patient outcomes PET—positron emission tomography, CT—computed tomography, PET/CT – fused images of PET and CT, MRI T2 FLAIR – Magnetic Resonance Image T2-weighted Fluid Attenuated Inversion Recovery, and IHC—immunohistochemical staining for PSMA of the tissue (PSMA antibody, mouse Mba, Dako/Agilent, Clone 3E6; dilution 1:50). A – A 31-year-old man with glioblastoma IDH-wildtype WHO 4 high-intensity accumulations of PSMA according to PET (PET, CT, PET/CT – arrows) with a strong reaction at low power at vessels and negative tumour cell staining (IHC, arrows). B – A 71-year-old woman with glioblastoma IDH-wildtype WHO 4 was diagnosed only by the NGS result (TERT mutation, tetrasomy of 7. and monosomy of 10. chromosome) and lack of PSMA accumulation in PET scans, with a visible lesion on CT (PET, CT, PET/CT – arrows) and a strong reaction at low power in the tumour tissue and negative staining of vessels (IHC, arrows). C – 34-year-old man with astrocytoma IDH-mutant WHO 4 with accumulation of PSMA in PET scans (PET, CT, PET/CT – arrows) with faint and weak staining at high vessel power and strong reaction at low tumour tissue staining power (IHC, arrows). D – A 31-year-old woman with astrocytoma IDH-mutant WHO 3—lack of PSMA accumulation in PET scans, with a visible lesion on CT (PET, CT, PET/CT – arrows) with moderate intensity staining at low power of the tumour tissue and negative staining of vessels (IHC, arrows).

[⁶⁸ Ga]Ga-PSMA-11 PET/CT positive	Sensitivity [%] (95% CI)	Specificity [%] (95% CI)	PPV [%] (95% CI)	NPV [%] (95% CI)	LR+ (95% CI)	LR- (95% CI)	DOR (95% CI)
WHO G4+G3	71.4 (51.3–86.8)	100.0 (79.4–100.0)	100.0 (83.1–100.0)	66.7 (44.7–84.4)	-	0.3 (0.2–0.5)	-
WHO G4	81.3 (54.4–96.0)	75.0 (55.1–89.9)	65.0 (40.8–84.6)	87.5 (67.6–97.3)	3.2 (1.6–6.4)	0.3 (0.1–0.7)	13 (2.9–59.4)
GBM IDH-wildtype	78.5 (49.2–95.3)	70.0 (50.6–85.2)	55.0 (31.5–76.9)	87.5 (67.6–97.3)	2.6 (1.4–4.8)	0.3 (0.1–0.9)	8.6 (1.9–38.2)

Table 1. Results of the qualitative analysis.

AUC (95% CI; cut-off)	GBM vs other diagnoses	WHO G4 vs G3 + G2
SUVmax	0.79 (0.65–0.94; 4.4)	0.84 (0.70–0.97; 4.4)
SUVmean	0.79 (0.64–0.94; 2.4)	0.83 (0.70–0.96; 2.4)
Volume	0.78 (0.63–0.93; 3.3)	0.83 (0.70–0.96; 12.3)
TBR	0.81 (0.66–0.96; 42.2)	0.84 (0.71–0.97; 42.2)
TLR	0.79 (0.64–0.94; 0.8)	0.73 (0.70–0.96; 0.8)

Table 2. Statistical results of quantitative analysis.

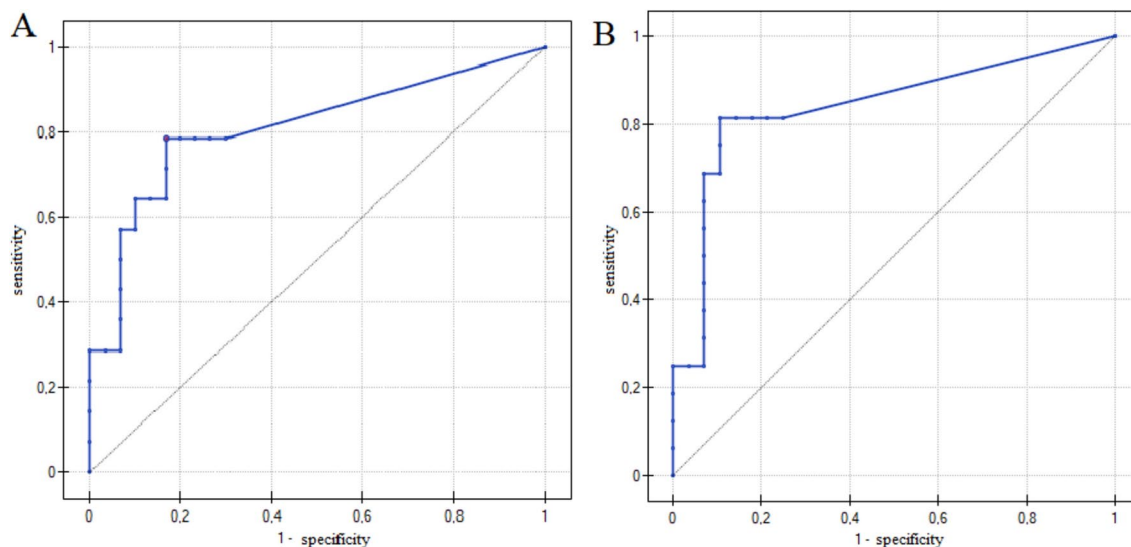


Fig. 4. The ROC curves with the AUC values: **A**—GBM vs other diagnoses—TBR 0.81 (0.66–0.96; 42.2) (95% CI; cut-off), **B**—WHO G4 vs G3 + G2—TBR 0.84 (0.71–0.97; 42.2) (95% CI; cut-off).

Quantitative analysis

To determine the best indicator for diagnosis, a comparison of the semiquantitative results of [^{68}Ga]Ga-PSMA-11 PET with those of histological examination was performed. The SUVmax, SUVmean, volume of the tumour foci, TBR and TLR were chosen as indicators against which the cut-off points for the given comparisons were determined using receiver operating characteristic (ROC) curves.

The results of the quantitative analysis were the same as those of the qualitative analysis for differentiating between HGG and LGG, which resulted from the diagnosis of HGG in all PET positive patients.

The area under the curve (AUC) values for GBM vs other diagnoses and for WHO G4 vs G3 + G2 tumours are shown in Table 2. For both groups, the highest AUC was obtained for TBR; however, there was no significant difference between the obtained field values according to the chart for other parameters. The ROC curves for the TBR are presented in Fig. 4.

Comparison with pre-surgical MRI

The analysis analysed the results of preoperative MRI, and PET compared to the final histopathological diagnosis in terms of the malignancy of the diagnosed lesion (HGG vs LGG). MRI showed concordance in 39 patients (89% agreement). Among these, MRI underestimated 2 cases of GBM and overestimated 2 cases of oligodendroglioma and astrocytoma. PET showed concordance with the final diagnosis in 36 patients (82% agreement). This study underestimated 3 cases of GBM (including the same 2 as MRI) and 3 cases of astrocytoma and 2 cases of oligodendroglioma. No overestimation of more malignant diagnoses was found for this study. It is worth mentioning that underdiagnosed GBM patients on PET had this diagnosis made only through genetic testing.

Immunohistochemistry analyses

Immunohistochemical staining for PSMA was performed in 39 patients. The samples from 5 patients did not contain enough material for additional immunohistochemical staining.

Immunohistochemical staining was noted in two compartments: tumour cells and blood vessels. In contrast to cell staining, positive vascular staining was associated with increased accumulation in the PET study. There was a significant correlation between the qualitative assessment of PSMA immunohistochemical staining of vessels and the qualitative assessment of [^{68}Ga]Ga-PSMA-11 PET/CT ($p < 0.00001$).

For the quantitative parameters, there was a positive correlation between the degree of vessel staining and the SUVmax ($p < 0.000001$) and a negative correlation between PSMA staining in tumour tissue and the SUVmax ($p < 0.001-0.000077$). The data are presented in Fig. 5.

Follow-up analyses

Till now, we performed at least 2-years follow-up after surgery, for each patient qualified for the study. The data were analysed based on the final histopathological results (GBM vs non-GBM, HGG vs LGG), the quantitative PET parameters (positive (PET+) and negative (PET-)) and the qualitative parameter with the best parameters (TBR with cut-off 42.2): positive (TBR+) and negative (TBR-). Additionally the suspected result of pre-surgical MRI were included in the analysis (MRI LGG and MRI HGG). The median PFS and OS times with SDs are listed in supplementary material 4. For all groups, the Kaplan–Meier estimator was calculated and compared via relevant statistical tests.

There was a significant difference in both PFS and OS between the variables for each group (GBM vs non-GBM, HGG vs LGG, PET+ vs PET-, TBR+ vs TBR-, MRI LGG vs MRI HGG). The median PFS and OS times were not reached during follow-up in all “negative” groups, namely, the non-GBM, LGG, PET-, TBR- and MRI LGG groups; moreover, there were no significant differences between those groups. In contrast, the other groups had worse results, with the worst result of only 199 days of PFS in the GBM and TBR+ cohorts (OS 318 and 424.5, respectively). Similarly, there were no significant differences between the “positive” groups: GBM, HGG, PET+, TBR+ and MRI HGG. The Kaplan–Meier estimator curves are presented in supplementary material 5.

When analysing the data, we found that the PET/CT with [^{68}Ga]Ga-PSMA-11 result in GBM patients differentiated patients in terms of prognosis, both in terms of progression-free survival and overall survival. Despite the small number of patients with a negative PET/CT result, statistically significant differences were found. The results are presented in Fig. 6.

Discussion

Primary glial tumours are a clinically significant problem due to their highly infiltrative character and inherent risk of recurrence despite aggressive surgical and oncological treatments. Timely diagnosis and management are especially important for HGG patients due to their rapid growth and short survival time; thus, preoperative differentiation between LGG and HGG is crucial. In both groups, detailed preoperative imaging information was important for surgical and oncological planning. Brain MRI is the first-choice imaging modality for evaluating patients with gliomas²⁶, as it plays a primary role in determining the location and involvement of the surrounding tissues²⁷. Despite advances in MRI techniques and different new modalities, accurate preoperative diagnosis of brain tumours is still a challenge²⁸.

The usefulness of PET with PSMA-targeting radiopharmaceuticals was demonstrated in imaging tumours of glial origin^{22,29}. These studies suggest that, irrespective of the radioactive tracer subtype or isotope used, the labelling of PSMA derivatives gives comparable results. Uptake of PSMA-targeting radiopharmaceuticals was detected in oligodendrogliomas^{30,31}, LGG progression to HGG³², residual GBM after surgery³³ and, especially, GBM recurrence^{20,34}. Kunikowska et al. examined PSMA expression in glioma recurrence using [^{68}Ga]Ga-PSMA-11 PET/CT, which revealed HGG and GBM recurrence^{9,24}. They found a 100% spatial correlation

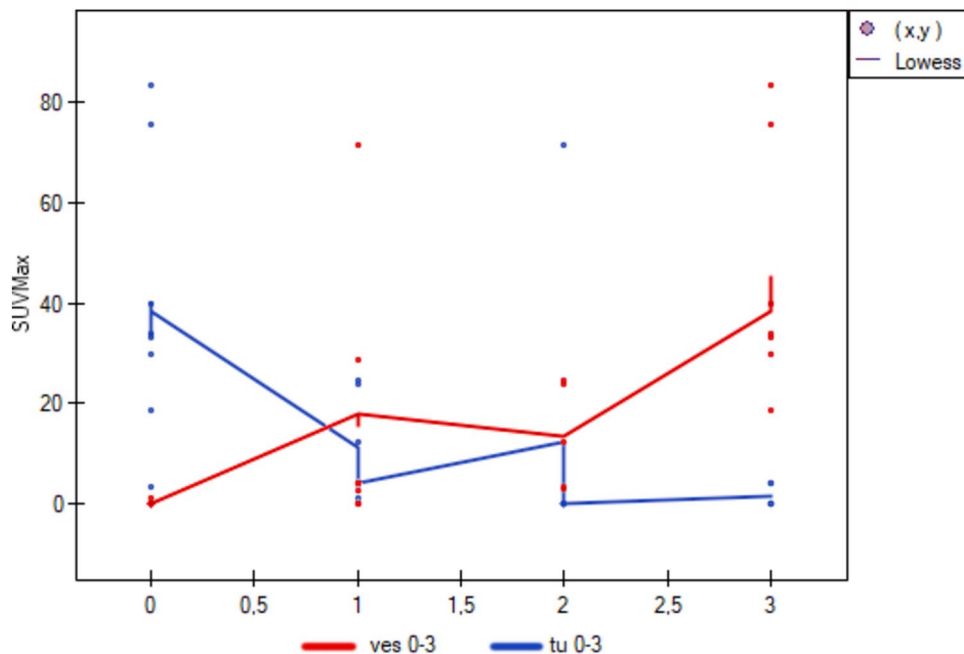


Fig. 5. Effect of the immunochemical staining intensity on the SUVmax. The red graph represents vascular staining, and the blue graph represents tumour tissue staining.

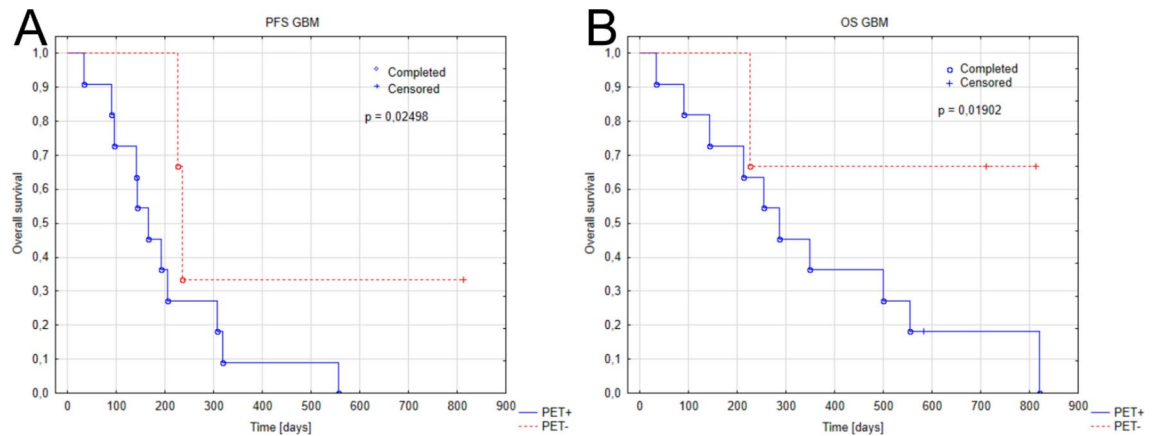


Fig. 6. Kaplan-Meier estimator curves for PFS (A) and OS (B) for the GBM patients in terms of positive and negative PSMA accumulation in PET/CT study.

between [^{68}Ga]Ga-PSMA-11 uptake and contrast enhancement areas on MRI. In all the patients, high TBR values were identified, with medians of 96.7 (32.2–357.5)²⁴ and 152 (15–1400)⁹. Sasikumar et al. reported very good contrast between lesions and background, with TBR values ranging from 4.07 to 29.4 in patients with suspected recurrence of GBM^{3,4}. In our study, high TBR values were recorded in all patients with a positive lesion; therefore, our results are consistent with the literature. The absence of PSMA uptake in the background indicates a high degree of differentiation between the tumour and the normal brain tissue. This feature may be useful during surgical resection because PET/CT can be easily fused with MRI and used in the setting of image-guided resection. However, the role of PSMA PET/CT-guided resection and its impact on survival time need further study.

In our study, [^{68}Ga]Ga-PSMA-11 PET/CT showed good specificity in differentiating HGG from LGG. Verma et al. reported similar results in 10 patients with suspected gliomas with higher SUVmax and TBR values in GBM than in LGG, although no specific information regarding tumour histopathology was given⁵. Akgun et al., in a study conducted on 42 lesions, identified a correlation between the SUVmax on PET/MR images and [^{68}Ga]Ga-PSMA-11 and between the SUVmax and the results of histopathological examination⁶. These authors were able to differentiate G2 + G3 from G4 with a cut-off of 2.3 (sensitivity 80%, specificity 81.8), which is consistent with our results, and to differentiate LGG from HGG with a cut-off of 1.15 (sensitivity 85.7%, specificity 85.7%). The estimated specificity is lower than that in our study, which can be explained by the limited genetic verification of the histopathological results and study group heterogeneity, as gliomas encompass other tumours apart from diffuse adult gliomas. Liu et al. examined the advantages of [^{68}Ga]Ga-PSMA-617 over [^{18}F]FDG PET/CT in the differentiation of HGG from LGG in a study of 30 patients⁷. The authors identified the [^{68}Ga]Ga-PSMA-617 SUVmax cut-off as 2.21 with 81% sensitivity and 100% specificity, which is comparable to the findings of our study. As in our study, lesions were considered exclusively diffuse adult gliomas, although only 86% of the diagnoses were confirmed by genetic testing. Microvascular proliferation and necrosis are hallmark histopathological features of WHO G4 tumours like GBM, IDH-wildtype¹³. In our study, these features were present in all GBM patients with PSMA uptake. In patients with GBM without PSMA uptake no microvascular proliferation or necrosis was detected and the diagnosis was based on the molecular features. In our study, [^{68}Ga]Ga-PSMA-11 PET/CT showed good sensitivity and specificity in differentiating glioblastoma IDH-wildtype from other diffuse gliomas. The good diagnostic properties of PET imaging with PSMA-targeting radiopharmaceuticals for HGG diagnosis were confirmed in a recent meta-analysis by Muoio et al.²³

PSMA expression on GBM vessels was confirmed by immunohistochemistry in all 32 patients examined by Wernicke³⁵ and 16 patients examined by Holzgrave³⁶. Nomura et al. examined the immunohistochemistry results of 19 gliomas of different grades and detected PSMA expression on all G4 tumour vessels, no staining on normal brain vessels and weak staining of some tumour cells in G2–G3 gliomas³⁷. In contrast, Mahzouni et al. reported positive staining for PSMA in 66% of 60 patients³⁸, and Saffar et al. reported positive staining for PSMA in 33.3% of HGGs vs 8.3% of LGGs in a study of 72 patients³⁹. The differences in the results of PSMA immunohistochemistry could be explained by the antibody used—studies using the primary mouse antibody mAb 3E6 showed 100% positive staining for GBM vessels^{35–37}, whereas others did not. In our study, PSMA immunohistochemistry was performed using the mouse antibody 3E6, and [^{68}Ga]Ga-PSMA-11 uptake was correlated with positive staining for PSMA on tumour vessels. The observed lack of tracer accumulation in 3 GBM patients and the lack of antibody staining in these patients requires further analysis. In contrast to PET/CT, retrospective IHC staining is possible, and is planned, on a larger group of patients.

The survival time of patients with gliomas is strongly related to histopathological results⁴⁰. LGG patients have a better prognosis, with survival averaging approximately 7 years⁴¹, while GBM patients' median survival time is 15 months, even after the best available treatment. Holzgrave et al. presented similar findings depending on the PSMA vessels expression in immunohistochemical staining³⁶. The patients with high level of vascular staining at recurrence had worse survival compared to patients with either low or decreasing staining level (12 vs 22 months). Despite only 1-year of follow-up, Kaplan-Meier curves confirmed the worst prognosis for patients

diagnosed with GBM, which is very close to a high TBR. The result of PET/CT with PSMA, especially with quantification of the tracer accumulation in the tumour compared to the background, proves to be a significant factor in determining the prognosis of the patient in a similar way to the histopathological result. We reached similar survival and disease progression times for GBM patients like literature. The accumulation of tracer in the PET scan was comparable to the immunohistochemical stains performed and is clearly a poor prognostic factor. Unfortunately, due to the short duration of the analysis, we were not able to identify all the variables. Further follow-up for at least 5-years is planned.

Ninatii et al. presented an interesting paper on the prognostic impact of the accumulation of [¹¹C]methionine in PET/CT study in patients with IDH-wildtype diffuse gliomas with histological features of lower-grade gliomas⁴². In this study the positive accumulation of the MET in the tumour was associated with statistically significant shorter median PFS and OS time. In our study, we noticed a similar correlation in terms of tracer corning in the group of patients with abscessed GBM. These were patients in whom a definitive diagnosis was made on the basis of genetic testing alone. Due to the rather short follow-up time, we do not know the impact of PSMA accumulation on the prognosis of patients with tumours other than GBM.

Our study has certain limitations. Although this study contains the largest number of included patients compared to the literature, statistically one of the limitations is still the number of patients. The study was conducted as a pilot study due to the lack of data about the power and strength of the test used. Only patients with a high suspicion of glioma in previous imaging studies were included; as a result, it was not possible to determine the primary sensitivity and specificity of the test. Another important limitation is the patient selection bias. For organisational reasons, it was not possible to perform the PET/CT examination in a group of consecutive patients presenting for neurosurgery. During the recruitment period, we were able to perform the study in less than 40% of the operated patients. Patients qualified for the study were matched in such a way that the additional examination could be performed at a safe time for them. Although the gender and age structure is similar to the overall group, we do not know the impact of selection bias on the final results of the study. This study may also be limited by the lack of histopathological data correlated with spatial location within heterogeneous tumours, e.g., from tumour regions with uptake of PSMA. During surgical resection of glial tumours, the acquired tissue is labelled according to its macroscopic appearance, as the shift in intracranial structures after craniotomy and the piecemeal manner of resection result in inaccuracies in correlation with preoperative imaging. This limitation could be overcome by performing a stereotactic or navigated biopsy, but this technique is not used routinely for patients for whom resection is planned. Another limiting factor is the observation period of at least 2-years — a sufficient time to show differences in prognosis between GBM patients and [⁶⁸Ga]Ga-PSMA-11-positive lesions—while further observation will be carried out to perform a multivariate survival analysis that also considers other quantitative and qualitative parameters, including patient data, surgical debulking, radiomic data on PET parameters not included so far and MRI findings.

Conclusions

Our study was conducted on the largest number of recruited patients with adult-type diffuse gliomas to date with histopathological diagnoses based on the latest WHO Classification of CNS tumours (2021) and supported by next-generation sequencing results. The study showed good specificity of [⁶⁸Ga]Ga-PSMA-11 PET/CT for the diagnosis of HGG and its promising sensitivity for histopathological features of GBM, such as microvascular proliferation. Due to the lack of tracer accumulation in healthy brain tissue, the diagnostic criteria are remarkably simple. A focus of high tracer accumulation corresponds to neovascularization, which may be useful in choosing an optimum site for histopathological material collection and may indicate progression from a less malignant tumour to a more malignant tumour. [⁶⁸Ga]Ga-PSMA-11 PET/CT is safe and well tolerated by patients. No side effects related to the radiopharmaceutical administration were found in this study.

Data availability

The data that support the findings of this study are not openly available due to reasons of sensitivity and are available from the corresponding author upon reasonable request.

Received: 19 August 2024; Accepted: 19 December 2024

Published online: 02 January 2025

References

- Horoszewicz, J. S., Kawinski, E. & Murphy, G. P. Monoclonal antibodies to a new antigenic marker in epithelial prostatic cells and serum of prostatic cancer patients. *Anticancer. Res.* **7**, 927–935 (1987).
- Farolfi, A. et al. Current and emerging clinical applications of PSMA PET diagnostic imaging for prostate cancer. *J. Nucl. Med.* **62**, 596–604. <https://doi.org/10.2967/jnumed.120.257238> (2021).
- Sasikumar, A. et al. Diagnostic Value of 68Ga PSMA-11 PET/CT imaging of brain tumors-preliminary analysis. *Clin. Nucl. Med.* **42**, e41–e48. <https://doi.org/10.1097/RLU.0000000000001451> (2017).
- Sasikumar, A. et al. Utility of 68Ga-PSMA-11 PET/CT in imaging of glioma—a pilot study. *Clin. Nucl. Med.* **43**, e304–e309. <https://doi.org/10.1097/RLU.0000000000002175> (2018).
- Verma, P. et al. Differential uptake of 68Ga-PSMA-HBED-CC (PSMA-11) in low-grade versus high-grade gliomas in treatment-naïve patients. *Clin. Nucl. Med.* **44**, e318–e322. <https://doi.org/10.1097/RLU.0000000000002520> (2019).
- Akgun, E., Akgun, M. Y., Selcuk, H. H., Uzan, M. & Sayman, H. B. (68)Ga PSMA PET/MR in the differentiation of low and high grade gliomas: Is (68)Ga PSMA PET/MRI useful to detect brain gliomas?. *Eur. J. Radiol.* **130**, 109199. <https://doi.org/10.1016/j.ejrad.2020.109199> (2020).
- Liu, D. et al. PET/CT using (68) Ga-PSMA-617 versus (18) F-fluorodeoxyglucose to differentiate low- and high-grade gliomas. *J. Neuroimaging* **31**, 733–742. <https://doi.org/10.1111/jon.12856> (2021).
- Kumar, A. et al. Ga-68 PSMA PET/CT in recurrent high-grade gliomas: Evaluating PSMA expression in vivo. *Neuroradiology* **64**, 969–979. <https://doi.org/10.1007/s00234-021-02828-2> (2022).

9. Kunikowska, J. et al. Expression of glutamate carboxypeptidase II in the glial tumor recurrence evaluated in vivo using radionuclide imaging. *Sci. Rep.* **12**, 652. <https://doi.org/10.1038/s41598-021-04613-w> (2022).
10. Pelka, K., Bodys-Pelka, A. & Kunikowska, J. Prostate-specific membrane antigen expression in intracranial lesions - a review of the primary, metastatic, and nonneoplastic lesions. *Nucl. Med. Rev. Cent. East Eur.* **26**, 134–142. <https://doi.org/10.5603/nmr.97019> (2023).
11. Rizzo, A. et al. PSMA radioligand uptake as a biomarker of neoangiogenesis in solid tumours: Diagnostic or theraagnostic factor?. *Cancers (Basel)* <https://doi.org/10.3390/cancers14164039> (2022).
12. Komori, T. Grading of adult diffuse gliomas according to the 2021 WHO classification of tumors of the central nervous system. *Lab. Invest.* **102**, 126–133. <https://doi.org/10.1038/s41374-021-00667-6> (2022).
13. Louis, D. N. et al. The 2021 WHO classification of tumors of the central nervous system: A summary. *Neuro. Oncol.* **23**, 1231–1251. <https://doi.org/10.1093/neuonc/noab106> (2021).
14. Brat, D. J. et al. cIMPACT-NOW update 3: Recommended diagnostic criteria for Diffuse astrocytic glioma, IDH-wildtype, with molecular features of glioblastoma, WHO grade IV. *Acta. Neuropathol.* **136**, 805–810. <https://doi.org/10.1007/s00401-018-1913-0> (2018).
15. Treglia, G., Sadeghi, R., Del Sole, A. & Giovannella, L. Diagnostic performance of PET/CT with tracers other than F-18-FDG in oncology: An evidence-based review. *Clin. Transl. Oncol.* **16**, 770–775. <https://doi.org/10.1007/s12094-014-1168-8> (2014).
16. Mattoli, M. V., T. G., Trevisi, G., Muoio, B. & Cason, E. Usefulness of 11c-methionine positron emission tomography in differential diagnosis between recurrent tumours and radiation necrosis in patients with glioma: An Overview. *Open Neurosurg. J.* **5**, 8–11. <https://doi.org/10.2174/187652970120501008> (2012).
17. Muoio, B., Giovannella, L. & Treglia, G. Recent developments of 18F-FET PET in neuro-oncology. *Curr. Med. Chem.* **25**, 3061–3073. <https://doi.org/10.2174/0929867325666171123202644> (2018).
18. van de Weijer, T. et al. The use of (18)F-FET-PET-MRI in neuro-oncology: The best of both worlds-a narrative review. *Diagnostics (Basel)* <https://doi.org/10.3390/diagnostics12051202> (2022).
19. Bertagna, E., B. G. & Giubbini, R. The role of F-18-fluorothymidine PET in oncology. *Clin. Transl. Imaging* **1**, 77–97. <https://doi.org/10.1007/s40336-013-0014-2> (2013).
20. Marafi, F., Sasikumar, A., Fathallah, W. & Esmail, A. 18F-PSMA 1007 brain PET/CT imaging in glioma recurrence. *Clin. Nucl. Med.* **45**, e61–e62. <https://doi.org/10.1097/RLU.0000000000002668> (2020).
21. Brighi, C. et al. Comparison between [68Ga]Ga-PSMA-617 and [18F]FET PET as imaging biomarkers in adult recurrent glioblastoma. *Int. J. Mol. Sci.* <https://doi.org/10.3390/ijms242216208> (2023).
22. van Lith, S. A. M. et al. PET imaging and protein expression of prostate-specific membrane antigen in glioblastoma: A multicenter inventory study. *J. Nucl. Med.* **64**, 1526–1531. <https://doi.org/10.2967/jnumed.123.265738> (2023).
23. Muoio, B. et al. Diagnostic accuracy of PET/CT or PET/MRI using PSMA-targeting radiopharmaceuticals in high-grade gliomas: A systematic review and a bivariate meta-Analysis. *Diagnostics (Basel)* <https://doi.org/10.3390/diagnostics12071665> (2022).
24. Kunikowska, J., Kulinski, R., Muylle, K., Koziara, H. & Krolicki, L. 68Ga-prostate-specific membrane antigen-11 PET/CT: A new imaging option for recurrent glioblastoma multiforme?. *Clin. Nucl. Med.* **45**, 11–18. <https://doi.org/10.1097/RLU.0000000000002806> (2020).
25. Vallejo-Armenta, P. et al. [(99m)Tc]Tc-iPSMA SPECT brain imaging as a potential specific diagnosis of metastatic brain tumors and high-grade gliomas. *Nucl. Med. Biol.* **96–97**, 1–8. <https://doi.org/10.1016/j.nucmedbio.2021.02.003> (2021).
26. Weller, M. et al. EANO guidelines on the diagnosis and treatment of diffuse gliomas of adulthood. *Nat. Rev. Clin. Oncol.* **18**, 170–186. <https://doi.org/10.1038/s41571-020-00447-z> (2021).
27. Cha, S. Update on brain tumor imaging. *Curr. Neurol. Neurosci. Rep.* **5**, 169–177. <https://doi.org/10.1007/s11910-005-0044-x> (2005).
28. Villanueva-Meyer, J. E., Mabray, M. C. & Cha, S. Current clinical brain tumor imaging. *Neurosurgery* **81**, 397–415. <https://doi.org/10.1093/neuros/nyx103> (2017).
29. Stopa, B. M. et al. Prostate-specific membrane antigen as target for neuroimaging of central nervous system tumors. *Mol. Imaging* **2022**, 5358545. <https://doi.org/10.1155/2022/5358545> (2022).
30. Pernthaler, B., Nazerani Hooshmand, T., Igreç, J., Kvaternik, H. & Aigner, R. M. Oligodendroglioma in 68Ga-PSMA-11 and 18F-Fluciclovine PET/CT. *Clin. Nucl. Med.* **46**, e231–e232. <https://doi.org/10.1097/RLU.0000000000003347> (2021).
31. Zhang, X., Yuan, J., Zhou, C. & Fan, W. Diagnose of glioma using 68Ga-PSMA and 18F-FDG PET/MRI. *Jpn. J. Clin. Oncol.* **51**, 506–508. <https://doi.org/10.1093/jjco/hyaa109> (2021).
32. Salas Fragomeni, R. A. et al. Prostate-specific membrane antigen-targeted imaging with [18F]DCFPyL in high-grade gliomas. *Clin. Nucl. Med.* **42**, e433–e435. <https://doi.org/10.1097/RLU.0000000000001769> (2017).
33. Pilati, E. et al. 68Ga-prostate-specific membrane antigen 11 PET/ct detects residual glioblastoma after radical surgery in a patient with synchronous recurrent prostate cancer: A case report. *Clin. Nucl. Med.* **45**, e151–e153. <https://doi.org/10.1097/RLU.0000000000002884> (2020).
34. Kumar, A. et al. 177Lu-/68Ga-psma theranostics in recurrent glioblastoma multiforme: Proof of concept. *Clin. Nucl. Med.* **45**, e512–e513. <https://doi.org/10.1097/RLU.00000000000003142> (2020).
35. Wernicke, A. G. et al. Prostate-specific membrane antigen as a potential novel vascular target for treatment of glioblastoma multiforme. *Arch. Pathol. Lab. Med.* **135**, 1486–1489. <https://doi.org/10.5858/arpa.2010-0740-OA> (2011).
36. Holzgreve, A. et al. PSMA expression in glioblastoma as a basis for theranostic approaches: A retrospective, correlational panel study including immunohistochemistry, clinical parameters and PET imaging. *Front. Oncol.* **11**, 646387. <https://doi.org/10.3389/fonc.2021.646387> (2021).
37. Nomura, N. et al. Prostate specific membrane antigen (PSMA) expression in primary gliomas and breast cancer brain metastases. *Cancer Cell. Int.* **14**, 26. <https://doi.org/10.1186/1475-2867-14-26> (2014).
38. Mahzouni, P. & Shavakhi, M. Prostate-specific membrane antigen expression in neovasculature of glioblastoma multiforme. *Adv. Biomed. Res.* **8**, 18. https://doi.org/10.4103/abr.abr_209_18 (2019).
39. Saffar, H., Noohi, M., Tavangar, S. M., Saffar, H. & Azimi, S. Expression of prostate-specific membrane antigen (PSMA) in brain glioma and its correlation with tumor grade. *Iran. J. Pathol.* **13**, 45–53 (2018).
40. Brown, N. F. et al. Survival outcomes and prognostic factors in glioblastoma. *Cancers (Basel)* <https://doi.org/10.3390/cancers14133161> (2022).
41. Claus, E. B. et al. Survival and low-grade glioma: The emergence of genetic information. *Neurosurg. Focus.* **38**, E6. <https://doi.org/10.3171/2014.10.FOCUS12367> (2015).
42. Ninatti, G. et al. The prognostic power of [(11)C]methionine PET in IDH-wildtype diffuse gliomas with lower-grade histological features: Venturing beyond WHO classification. *J. Neurooncol.* **164**, 473–481. <https://doi.org/10.1007/s11060-023-04438-9> (2023).

Acknowledgements

We would like to thank Paweł Włodarski, Head of Laboratory of Centre for Preclinical Research, Department of Research Methodology, Medical University of Warsaw, Warsaw, Poland for preparing and providing Figure 1.

Author contributions

The study conception and design J. Kunikowska; K. Pełka, L. Królicki and P.Kunert. Material preparation and data collection K. Pełka, K. Koczyk, L. Koperski, T. Dziedzic, A. Nowak, and J. Kunikowska; data analysis were performed by K. Pełka. Graphic illustration K. Pełka and L. Koperski. L.Królicki critically revised the manuscript for intellectual content. The first draft of the manuscript was written by K. Pełka and K. Koczyk and all authors commented on previous versions of the manuscript. All authors read and approved the final manuscript.

Funding

This work was performed as part of the Project "Predictive values of preoperative [⁶⁸Ga]Ga-PSMA-11 PET/CT in patients with suspected brain tumours of glial origin", number 1W13/1/M/MB/N/23, carried out from 2023 to 2024, funded by a subvention for science obtained by the Medical University of Warsaw.

Declarations

Competing interests

JK reports participation on a Data Safety Monitoring Board and Advisory Board from Novartis (personal fees); lecture honoraria from Monrol The other authors have no competing interests as defined by Nature Research, or other interests that might be perceived to influence the results and/or discussion reported in this paper.

Ethics approval

This study was performed in accordance with the principles of the Declaration of Helsinki. Approval was granted by the Ethics Committee of the Medical University of Warsaw (KB/2/A/2018 and KB/177/2021). Informed consent was obtained from all individual participants included in the study. Written informed consent was obtained from all patients. The study has been registered at clincialtrials.gov (number: NCT05896449) at 09/06/2023.

Additional information

Supplementary Information The online version contains supplementary material available at <https://doi.org/10.1038/s41598-024-84036-5>.

Correspondence and requests for materials should be addressed to K.P.

Reprints and permissions information is available at www.nature.com/reprints.

Publisher's note Springer Nature remains neutral with regard to jurisdictional claims in published maps and institutional affiliations.

Open Access This article is licensed under a Creative Commons Attribution-NonCommercial-NoDerivatives 4.0 International License, which permits any non-commercial use, sharing, distribution and reproduction in any medium or format, as long as you give appropriate credit to the original author(s) and the source, provide a link to the Creative Commons licence, and indicate if you modified the licensed material. You do not have permission under this licence to share adapted material derived from this article or parts of it. The images or other third party material in this article are included in the article's Creative Commons licence, unless indicated otherwise in a credit line to the material. If material is not included in the article's Creative Commons licence and your intended use is not permitted by statutory regulation or exceeds the permitted use, you will need to obtain permission directly from the copyright holder. To view a copy of this licence, visit <http://creativecommons.org/licenses/by-nc-nd/4.0/>.

© The Author(s) 2024